PCCP

PAPER

View Article Online
View Journal | View Issue

Cite this: *Phys. Chem. Chem. Phys.*, 2015, **17**, 19929

Boronyl as a terminal ligand in boron oxide clusters: hexagonal ring C_{2v} B_6O_4 and ethylene-like D_{2h} $B_6O_4^{-/2-}$†

Wei Wang,[a] Qiang Chen,[a] Ying-Jin Wang,[a] Hui Bai,[a] Ting-Ting Gao,[a] Hai-Ru Li,[a] Hua-Jin Zhai*[ab] and Si-Dian Li*[a]

Received 9th February 2015,
Accepted 29th June 2015

DOI: 10.1039/c5cp00812c

www.rsc.org/pccp

Considerable recent research effort has been devoted to the development of boronyl (BO) chemistry. Here we predict three perfectly planar boron boronyl clusters: C_{2v} B_6O_4 (**1**, $^1A_1$), D_{2h} $B_6O_4^-$ (**2**, $^2B_{3u}$), and D_{2h} $B_6O_4^{2-}$ (**3**, ^1A_g). These are established as the global-minimum structures on the basis of the coalescence kick and basin hopping structural searches and electronic structure calculations at the B3LYP/aug-cc-pVTZ level, with complementary CCSD/6-311+G* and single-point CCSD(T)/6-311+G*//B3LYP/aug-cc-pVTZ calculations for **2**. The C_{2v} B_6O_4 neutral cluster features a hexagonal B_4O_2 ring with two terminal BO groups. The D_{2h} $B_6O_4^{-/2-}$ clusters have ethylene-like structures and are readily formulated as $B_2(BO)_4^{-/2-}$, in which a B_2 core with double bond character is bonded to four terminal BO groups. Chemical bonding analyses show that B_6O_4 (**1**) possesses an aromatic π bonding system with three delocalized, six-centered π bonds over the hexagonal ring, rendering it an inorganic analogue of benzene, whereas the $B_6O_4^{-/2-}$ (**2** and **3**) species closely resemble ethylene in terms of structures and bonding. This work provides new examples for the analogy between boron oxides and hydrocarbons.

1. Introduction

Boron oxide clusters have recently emerged as fertile grounds for the discovery of novel molecular structures and chemical bonding.[1–5] The studies in this direction are primarily built on the accumulating knowledge of the structures and bonding of elemental boron clusters in the past decade, as a result of systematic, combined experimental and computational investigations.[6–20] As a prototypical electron-deficient element, boron clusters were shown to possess unique planar or quasi-planar (2D) structures over a wide range of sizes (B_n^- and B_n; n = 3–25, 30, 35 and 36).[21–38] A very recent paper reported the discovery of all-boron fullerenes or borospherenes $B_{40}^{0/-}$, the first free-standing boron cages, which are composed of interwoven boron double-chain ribbons, with two B_6 hexagon holes on the top and at the bottom and four B_7 heptagon holes on the waist.[39] This was closely followed by the observation/prediction[40,41] of chiral borospherenes $B_{39}^-/B_{41}^+/B_{42}^{2+}$ and theoretical predictions of the viability of a series of metalloborospherenes: endohedral M@B_{40} (M = Ca, Sr) and exohedral M&B_{40} (M = Be, Mg).[42] In all these boron clusters, the bonding is dominated by (σ and π) aromaticity and antiaromaticity,[43,44] where the electron delocalization helps compensate for boron's intrinsic electron-deficiency. Upon oxidation of boron clusters, the boron oxide clusters appear, which have long been considered to be the key to mechanistic understanding of the highly energetic combustion processes of boron and boranes at the molecular level.[3] Boron oxide clusters are even more electron-deficient with respect to the bare boron clusters, thus offering opportunities to explore exotic chemical bonding.

In boron oxide clusters, the BB bonding and BO bonding collectively govern their structural properties. The former features aromaticity/antiaromaticity as mentioned above, whereas the latter is dominated by the robust B≡O triple bond, that is, the boronyl group.[1] In boron-rich boron oxide clusters, the structures and bonding appear to be entirely dominated by the boronyl groups, where BO and BO^- are isoelectronic to the well-known inorganic ligands CN and CN^-/CO, respectively. The boronyl group can serve as a terminal, bridging, or face-capping ligand in boron oxide clusters and in metal boronyl complexes. Furthermore, the nature of boronyl as a monovalent σ radical allows the establishment of interesting analogy between boron oxide clusters and the boranes, in which

[a] *Nanocluster Laboratory, Institute of Molecular Science, Shanxi University, Taiyuan 030006, China. E-mail: hj.zhai@sxu.edu.cn, lisidian@sxu.edu.cn*
[b] *State Key Laboratory of Quantum Optics and Quantum Optics Devices, Shanxi University, Taiyuan 030006, China*

† Electronic supplementary information (ESI) available: Representative isomeric structures of $B_6O_4^{0/-/2-}$ along with their relative energies at the B3LYP/aug-cc-pVTZ level, selected canonical molecular orbitals (CMOs) of C_{2v} B_6O_4 (**1**, $^1A_1$) and D_{2h} $B_6O_4^-$ (**2**, $^2B_{3u}$), and the Wiberg bond indices of C_{2v} B_6O_4 (**1**, $^1A_1$). See DOI: 10.1039/c5cp00812c

a BO group is isolobal to H. The concept of BO/H isolobal analogy suggests the possibilities to rationally design new boron oxide clusters. For example, the linear $D_{\infty h}$ $B(BO)_2^{0/-}$, triangular D_{3h} $B(BO)_3^{0/-}$, and tetrahedral T_d $B(BO)_4^-$ species were recently characterized, which are perfect boron oxide analogues of the simplest boron hydride molecules: $BH_n^{0/-}$ (n = 2–4).[6–8,19]

By tuning the ratio of B *versus* O in the boron oxide clusters, one can also generate new chemical structures and uncover new types of chemical bonding. Among the studies along this line was the computational discovery[45,46] of the boronyl boroxine, D_{3h} $B_3O_3(BO)_3$, in which a boroxol B_3O_3 ring is surrounded by three BO groups. The boronyl boroxine was shown to be a close inorganic analogue of boroxine ($B_3O_3H_3$) and benzene, which all possess an aromatic π sextet. The B/O ratio in the six-membered ring aromatic core is 1 : 1 in boronyl boroxine and boroxine, same as that in the boroxol ring in glassy B_2O_3 bulk materials[47] and at high temperature B_2O_3 melts.[48] Heretofore, it remains unclear whether a heterocyclic six-membered B_mO_n ring with a B/O ratio other than 1 : 1 is feasible in boron oxides, and how the B/O ratio alters the aromaticity of the heterocyclic ring.

The current work is a continuation of our interest in the elucidation and design of new boron oxide clusters and boron boronyl complexes.[1,7–10,14,46] We report a theoretical study on a series of boron oxide clusters: C_{2v} B_6O_4 (**1**, $^1A_1$), D_{2h} $B_6O_4^-$ (**2**, $^2B_{3u}$), and D_{2h} $B_6O_4^{2-}$ (**3**, ^1A_g), which are identified as the global-minimum structures of the system *via* extensive global structural searches and electronic structure calculations at the B3LYP, CCSD, and single-point CCSD(T) levels. The B_6O_4 (**1**) neutral cluster is shown to possess a hexagonal B_4O_2 ring as the core, which has the B/O ratio of 2 : 1. This cluster turns out to be a new member of the "inorganic benzene" family. In contrast, the $B_6O_4^{-/2-}$ (**2** and **3**) species adopt ethylene-like open structures with a B_2 core and four terminal BO groups, rendering them the boron oxide analogues of ethylene. This work provides further examples for boronyl as a terminal ligand in boron oxides, and builds interesting connections between the boron oxides and the hydrocarbons.

2. Computational methods

Global-minimum structural searches for the $B_6O_4^{0/-/2-}$ clusters were carried out using the coalescence kick (CK)[49,50] and basin hopping (BH)[51] algorithms, initially at the B3LYP/3-21G level. The candidate low-lying structures were further optimized and frequency analyses were performed using the density functional theory (DFT) at the B3LYP/aug-cc-pVTZ level.[52] Additional calculations were carried out at the CCSD/6-311+G* level[53,54] and the CCSD(T)/6-311+G*//B3LYP/aug-cc-pVTZ to confirm the D_{2h} (**2**, $^2B_{3u}$) structure as a true minimum and hence the global minimum for $B_6O_4^-$; it is stressed that this included full structural optimization at the CCSD level. Chemical bonding analyses were accomplished using the adaptive natural density partitioning (AdNDP),[55] the canonical molecular orbitals (CMOs), and the nucleus independent chemical shift (NICS).[56,57] Photoelectron spectra of the $B_6O_4^-$ anion clusters were predicted using the time-dependent B3LYP (TD-B3LYP) method.[58] All calculations were done using the Gaussian 09 package.[59]

3. Results

On the basis of computational CK and BH structural searches and subsequent re-optimizations at the B3LYP/aug-cc-pVTZ level for $B_6O_4^{0/-/2-}$ and complementary CCSD/6-311+G* calculations for $B_6O_4^-$, we have established the global-minimum structures for B_6O_4 in three charge states: 0, −1, and −2. To further validate the performance of the B3LYP method for $B_6O_4^{0/-/2-}$ clusters, we re-optimized the structures of the top two or three isomers for each charge state at the PBE0/aug-cc-pVTZ level. The structures and energetics at B3LYP and PBE0 are highly consistent. Fig. 1 depicts these structures along with their bond distances at the B3LYP level. Alternative optimized low-lying structures are collected in Fig. S1–S3 in the ESI,† including their relative energies and minimum vibrational frequencies.

3.1. B_6O_4

The global-minimum structure at the B3LYP level for the neutral B_6O_4 cluster is C_{2v} (**1**, $^1A_1$), as shown in Fig. 1. It possesses a heterocyclic, hexagonal B_4O_2 ring as the core, with two BO groups attached terminally, which may be formulated as $B_4O_2(BO)_2$. The bond distances for terminal BO and terminal BB fall in the 1.202–1.207 and 1.621–1.667 Å range, typical for triple B≡O and single B–B bonds, respectively.[8] The BO and BB bonds within the hexagonal B_4O_2 ring are formally assigned as single B–O and B–B bonds, but their distances of 1.336–1.392 and 1.539 Å are markedly shorter than typical single bonds[8] due to the additional delocalized π system in the ring (see Section 4 for further discussion).

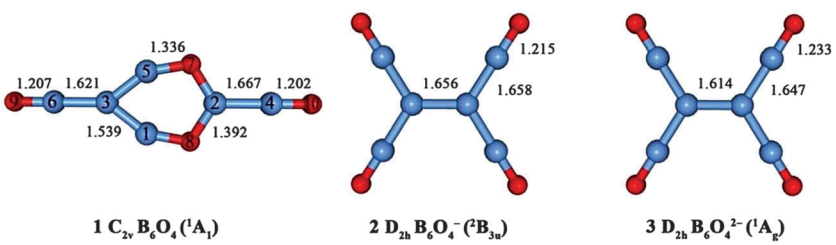

Fig. 1 Optimized cluster structures of C_{2v} B_6O_4 (**1**, $^1A_1$), D_{2h} $B_6O_4^-$ (**2**, $^2B_{3u}$), and D_{2h} $B_6O_4^{2-}$ (**2**, ^1A_g) at the B3LYP/aug-cc-pVTZ level. The bond distances (in Å) are labeled. B atom is in blue and O in red. See text for further discussion on $B_6O_4^-$ (**2**) at the B3LYP, CCSD, and CCSD(T) levels.

The second lowest isomer for B_6O_4 is 15.67 kcal mol^{-1} higher in energy at the B3LYP/aug-cc-pVTZ level (15.15 kcal mol^{-1} at the PBE0/aug-cc-pVTZ level), whereas alternative structures are at least $\sim$20 kcal mol^{-1} above the global minimum (Fig. S1 in the ESI†). This energetics information indicates that C_{2v} (**1**, $^1A_1$) is the well-defined global minimum on the potential energy surface.

3.2. $B_6O_4^-$

As shown in Fig. 1, the global minimum of the $B_6O_4^-$ monoanion is the (**2**, $^2B_{3u}$) state with D_{2h} symmetry. However, at the B3LYP/aug-cc-pVTZ level, the D_{2h} structure has one imaginary frequency of -12 cm^{-1} (Fig. S2 in the ESI†), which converts to a lower symmetry of D_2 upon further structural optimization. In the latter, the terminal BO groups undergo a slight out-of-plane twist around the B_2 core, by $\sim$17°. Similar structures, energetics, and vibrational properties are obtained for D_2 *versus* D_{2h} at the PBE0 level. We suspect that the tiny imaginary frequency may be an artifact of the DFT method being used. To resolve this technical issue, we have run full CCSD/6-311+G* structural optimization for the D_{2h} structure. Indeed, it turns out that the D_{2h} structure is a true minimum on the potential energy surface at the CCSD/6-311+G* level (minimum frequency: 19 cm^{-1}). As a further benchmark, single-point CCSD(T)/6-311+G*//B3LYP/aug-cc-pVTZ calculations indicate that the D_{2h} structure is 0.13 kcal mol^{-1} lower in energy than D_2. Based on these, we conclude that the true global minimum of the $B_6O_4^-$ monoanion has the D_{2h} symmetry. The lowest-lying isomer for $B_6O_4^-$, C_1 (^{2}A), has a triangular B_3 core and is located at 16.92 and 12.32 kcal mol^{-1} higher in energy at the B3LYP and PBE0 levels, respectively. Note that the energetics at B3LYP and PBE0 are again consistent with each other, and the global minimum of $B_6O_4^-$ (**2**, D_{2h}, $^2B_{3u}$) (Fig. 1) is again well defined. Among other optimized structures, the heterocyclic hexagonal ring structure, C_{2v} ($^2A_1$), is markedly higher in energy, being 17.36 kcal mol^{-1} above the global minimum (Fig. S2 in the ESI†), in sharp contrast to the neutral case (Fig. S1 in the ESI†).

The D_{2h} $B_6O_4^-$ (**2**, $^2B_{3u}$) global-minimum structure has a B_2 core, which is attached by four terminal BO groups (Fig. 1). All atoms are coplanar. The BB bond distance in the B_2 core is 1.656 Å at the B3LYP level, whereas the BB distance between the B_2 core and the BO groups is 1.658 Å. All these are comparable to that of a typical B–B single bond (although the BB bonding in the B_2 core has a formal bond order of 1.5).[8] The terminal BO bond distance is 1.215 Å, which is typical for a B$\equiv$O triple bond.

3.3. $B_6O_4^{2-}$

The global minimum of the $B_6O_4^{2-}$ dianion is D_{2h} (**3**, ^1A_g) (Fig. 1); see also Fig. S3 in the ESI.† This structure is rather similar to the D_{2h} (**2**, $^2B_{3u}$) global minimum of the $B_6O_4^-$ monoanion. The BB bond distance in the B_2 core shrinks by 0.04 Å from **2** to **3**, despite the increase of intramolecular coulomb repulsion in the latter species. Again, the BO bond distance for the four terminal BO groups is 1.233 Å, typical for a B$\equiv$O triple bond. Alternative structures for the dianion are at least 28.39 and 19.56 kcal mol^{-1} higher in energy at the B3LYP and PBE0 levels, respectively (Fig. S3, ESI†), suggesting that the global minimum for the $B_6O_4^{2-}$ dianion is well defined on the potential energy surface.

4. Discussion

4.1. B_6O_4: heterocyclic hexagonal B_4O_2 ring and inorganic analogue of benzene

The hexagonal boroxol B_3O_3 ring is generally considered as the dominant structural block in amorphous B_2O_3 bulk materials,[47] and at high temperature B_2O_3 melts,[48] as well as in the boroxine D_{3h} $B_3O_3H_3$ and the recently discovered boronyl boroxine, D_{3h} $B_3O_3(BO)_3$.[46] In all these, the B/O ratio in the six-membered BO ring is 1:1, which gives rise to symmetric, heterocyclic structures. In particular, both the boroxine D_{3h} $B_3O_3H_3$ and the boronyl boroxine D_{3h} $B_3O_3(BO)_3$ possess six delocalized π electrons, rendering them inorganic analogues of benzene. The neutral B_6O_4 cluster offers another six-membered BO ring system, C_{2v} (**1**, $^1A_1$), albeit with a different B/O ratio of 2:1.

Being attached by two BO groups *via* B–B single bonds (Fig. 1), the B_4O_2 ring in **1** has effectively six valence electrons for the global bonding when one assumes that all BB and BO bonds in the B_4O_2 ring are single bonds: of the 24 valence electrons, two are used to form terminal BB bonds, 12 are for the BB and BO single bonds in the ring, and 4 are the O lone pairs. This simple electron counting appears to be correct. The CMO analysis shows indeed three delocalized π CMOs: HOMO(b_1), HOMO$-$10(a_2), and HOMO$-$12(b_1) (Fig. S4 in the ESI†). Similar π orbitals are also revealed in the AdNDP analysis (Fig. 2a), which are six-center two-electron (6c-2e) in nature, globally covering the B_4O_2 ring. This π sextet is rather similar to that in benzene (Fig. 2b), rendering the B_6O_4 C_{2v} (**1**, $^1A_1$) cluster a new member of the inorganic benzene family.

Different from benzene, and from boroxine and boronyl boroxine[45] as well, the distribution of π electron cloud in **1** is heavily uneven within the B_4O_2 ring. The bonding in benzene shows true six-centered delocalization. Orbital composition analyses for **1** show that HOMO(b_1) is primarily composed of the B 2p_z atomic orbitals (AOs) from B1, B5, and B3 (see Fig. 1 from the labels of atoms) by 23%, 23%, 35%, respectively, which amounts to 81% in total. On the other hand, HOMO$-$10(a_2) contains almost pure contributions of O 2p_z AOs from O7 (48%) and O8 (48%), whereas HOMO$-$12(b_1) involves mainly B 2p_z AO from B2 and O 2p_z from O7 and O8, which are 10%, 39%, and 39%, respectively. The combination of HOMO$-$10 and HOMO$-$12 recovers 87% O 2p_z component on both O7 and O8, suggesting that these two CMOs essentially originate from the O 2p_z lone pairs, as anticipated. In effect, the B_4O_2 ring in **1** may be alternatively viewed as the fusion of a B_3 ring and a B_3O_2 ring, as illustrated in Fig. S5 in the ESI,† where the B_3 ring is a highly delocalized 2π subsystem. Overall, the extent of six-membered π delocalization in **1** is limited, similar to that in boroxine D_{3h} $B_3O_3H_3$ and boronyl boroxine D_{3h} $B_3O_3(BO)_3$.[46] Nonetheless, the larger B/O ratio of the heterocyclic BO ring in **1** makes it slightly more aromatic than the latter species.

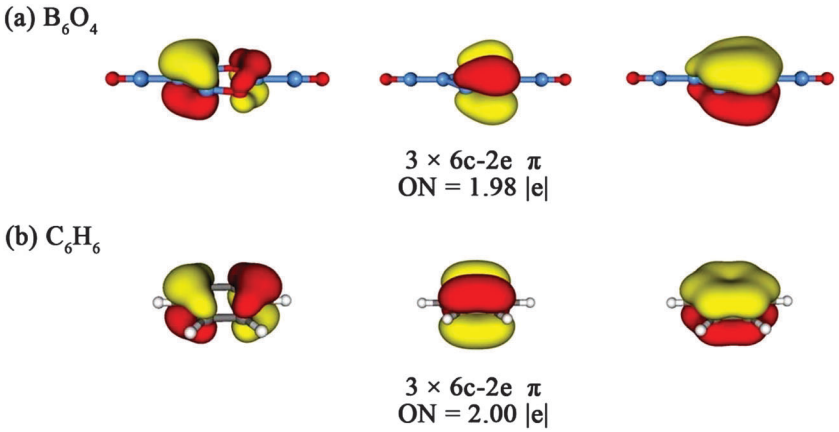

Fig. 2 Comparison of the delocalized π canonical molecular orbitals (CMOs) from the adaptive natural density partitioning (AdNDP) analyses for (a) B_6O_4 (**1**) and (b) benzene.

NICS is widely used to quantify the aromaticity and a negative NICS value denotes aromaticity. We choose to calculate $NICS_{zz}(1)$ at the center of the B_4O_2 ring and the center of the three B atoms in **1**, which are −7.17 and −15.29 ppm, respectively. These values correlate closely with the nature of electron delocalization in the ring as discussed above, showing that the extent of aromaticity varies from domain to domain in the ring. Thus one can tune the aromaticity in the BO systems *via* the change of B *versus* O ratio. For comparison, the prototypical aromatic benzene has a $NICS_{zz}(1)$ value of −29.69 ppm at the same level.

4.2. $B_6O_4^{-/2-}$: B–B multiple bonds, terminal BO groups, and the BO/H isolobal analogy

Our previous studies on the boron oxide clusters[6–14,46] have shown the structural and chemical integrity of the boronyl group as a key structural unit and have also established the close analogy between boron-rich oxide clusters and boranes, where the BO group as a robust monovalent σ radical is isolobal to H. In the current D_{2h} $B_6O_4^-$ (**2**) and $B_6O_4^{2-}$ (**3**) clusters, the terminal BO groups exhibit rigid bond distances of 1.215–1.233 Å (Fig. 1), which are characteristic of a B≡O triple bond. The bonds between the BO groups and the B_2 core, 1.647–1.658 Å, are roughly B–B single bonds. The above bond order assignments are perfectly borne out from the AdNDP analysis (Fig. 3a). The **2** and **3** species thus provide new examples for the robustness of the B≡O triple bond and further demonstrate boronyl as a monovalent σ radical ligand.

In terms of the bonding of the B_2 core in D_{2h} $B_6O_4^-$ (**2**) and $B_6O_4^{2-}$ (**3**), AdNDP reveals one 2c-2e σ bond and one 2c-2e π bond in the closed-shell **3** species (Fig. 3a), suggesting a formal

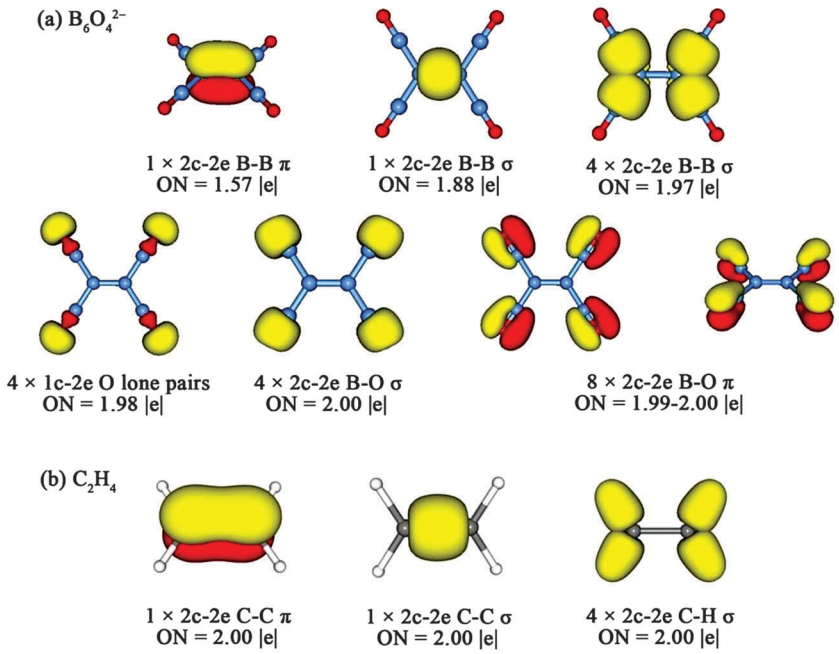

Fig. 3 Bonding elements as revealed from the AdNDP analyses for (a) $B_6O_4^{2-}$ (**3**) and (b) C_2H_4. The occupation numbers (ONs) are labeled.

B═B double bond. The B═B double bond can also be traced back to the CMOs. With one electron less than **3**, the open-shell **2** species has a singly occupied π HOMO, resulting in a formal bond order of 1.5 for the B_2 core (Fig. S4 in the ESI†).

For completeness, a typical B–B single bond may be found in the B_6O_4 (D_{2d}, $^1A_1$) species (Fig. S1 in the ESI†), which is a true minimum for B_6O_4 and located at ~20 kcal mol^{-1} above the global minimum. Thus, with the increase of formal bond order from 1.0 to 1.5 to 2.0, the bond distance in the B_2 core varies gradually: 1.635 Å in B_6O_4 (D_{2d}, $^1A_1$), 1.656 Å in **2**, and 1.614 Å in **3**. The latter two values indeed show a shrink in the bond distance with increasing bond order, but both these values are markedly longer than the anticipated distances[8] for a bond order of 1.5 or 2.0. The "abnormal" bond distances may be attributed to three factors: (i) the intramolecular coulomb repulsion in the anion and the dianion (**2** and **3**); (ii) the increasing repulsion between the four BO groups associated with their geometric changes to coplanarity; (iii) the conjugation of the six B atoms in **2** and **3**, which effectively increases the bond order in the terminal BB units and decreases that in the B_2 core.

It is immediately apparent that there is a structural connection between **2**/**3** and ethylene. Both systems are coplanar, featuring a diatomic core with a multiple bond and four terminal monovalent σ ligands. The essence of chemical bonding is also similar for the two systems. The diatomic core involves one σ bond plus one π bond (BB *versus* CC), and the link between the core and the ligands is accomplished *via* four terminal σ single bonds (B–BO *versus* C–H). This similarity is clearly depicted in Fig. 3, which is readily understandable. First, the BO group has recently been established as a monovalent σ radical,[1] isolobal to H. Second, B^- may be viewed as C *via* "electronic transmutation".[60] Thus, D_{2h} $B_6O_4^{2-}$ (**3**) and ethylene are exactly isovalent systems, which underlie their analogous structures.

4.3. Every electron counts: structural evolution from B_6O_4 to $B_6O_4^-$ to $B_6O_4^{2-}$

The evolution of the global-minimum structures of B_6O_4 (**1**), $B_6O_4^-$ (**2**), and $B_6O_4^{2-}$ (**3**) is remarkable, which demonstrates a key concept in cluster science: every electron counts. An in-depth elucidation of this evolution may be difficult, but we would like to offer our tentative explanation here. For the B_6O_4 neutral system, the hexagonal B_4O_2 ring has 24 valence electrons in total. Upon the removal of two electrons contributing to the peripheral B–BO bonds and two O 2p lone pairs, the B_4O_2 ring has 18 electrons for chemical bonding within the six-membered ring, which is equal to that of the C_6 ring in benzene. Thus the B_6O_4 neutral has the advantage to adopt the ring-like structure and to form a π sextet, where the aromatic delocalization helps stabilize the system.

Upon the addition of extra electrons to the system (such as in the cases of the $B_6O_4^-$ anion and the $B_6O_4^{2-}$ dianion), the electron counting becomes less ideal for the ring and alternative structures become competitive. In particular, the open structures $B_6O_4^-$ (**2**) to $B_6O_4^{2-}$ (**3**) offer the advantages to release the intramolecular coulomb repulsion *via* the four terminal BO groups. Furthermore, the open structures **2**/**3** may also facilitate the π conjugation across all six B atoms. Indeed, according to the AdNDP results (Fig. 3a), the occupation number (ON) for the 2c–2e π bond in **3** (1.57) is significantly smaller than the ideal value of 2.0, suggesting that the remaining four B atoms also contribute to this π bond. It is also worth noting that the structural twisting from D_{2d} B_6O_4 ($^1A_1$) (Fig. S1 in the ESI†) to D_{2h} $B_6O_4^-$ (**2**) and $B_6O_4^{2-}$ (**3**), where the partial delocalization of the BB π bond over all six B atoms is clearly the driving force to coplanarity in **2** and **3**.

4.4. Simulated photoelectron spectrum

To facilitate the forthcoming experimental characterization of these boron oxide clusters, we have calculated the ground-state vertical detachment energies (VDEs) of the $B_6O_4^-$ anion cluster at the B3LYP level, calculated their higher VDEs for the excited-state transitions using TD-B3LYP, and simulated the photoelectron spectra of both the ethylene-like D_{2h} $B_6O_4^-$ (**2**, $^2B_{3u}$) (Fig. 1) and the benzene analogue C_{2v} $B_6O_4^-$ ($^2A_1$) structures (Fig. S2 in the ESI†), the latter being associated with the neutral global minimum (**1**).

As shown in Fig. 4a, the D_{2h} $B_6O_4^-$ (**2**, $^2B_{3u}$) species has a predicted ground state VDE of 5.01 eV, followed by the first excited state at the VDE of 6.74 eV. The high first VDE suggests that the extra electron in the $B_6O_4^-$ (**2**) anion is strongly bound, consistent with the nature of the anion HOMO (Fig. S4 in the ESI†). Preliminary gas-phase photoelectron spectroscopic measurements reveal an experimental first VDE of 4.84 ± 0.05 eV for the $B_6O_4^-$ anion (H. J. Zhai and L. S. Wang, unpublished data), in good agreement with the current calculated value, which lends considerable credence to the anion global-minimum structure: D_{2h} $B_6O_4^-$ (**2**, $^2B_{3u}$). One reviewer of this manuscript thought that the DFT methods could overestimate the intramolecular coulomb repulsion for the anions and thus result in computational errors. This does not seem to be the case for the B3LYP calculations on **2**, because an overestimation of the coulomb repulsion for an anion should underestimate the VDE. However, the current calculated first VDE is slightly higher than the preliminary experimental measurement and yet within the anticipated uncertainties of the B3LYP method. Nonetheless, the reviewer suggested an interesting possibility of handling such systems using an alternative method, that is, the finite Hubbard model, where one can bring the DFT and the Hubbard model together.[61–65] It is unclear how good such calculations will work, but it is worthy of pursuit in the future.

In contrast, the calculated photoelectron spectrum of the benzene-like C_{2v} $B_6O_4^-$ ($^2A_1$) structure (Fig. 4b) shows a first VDE of 2.68 eV, which is markedly lower (by ~2.3 eV) than that of D_{2h} $B_6O_4^-$ (**2**, $^2B_{3u}$). This difference decisively overturns the energy order of the ethylene-like *versus* benzene-like structures in the anion state with respect to the neutral state. Note also that the calculated first VDE of C_{2v} $B_6O_4^-$ ($^2A_1$) deviates significantly from the preliminary experimental data mentioned above, consistent with the calculated relative energies

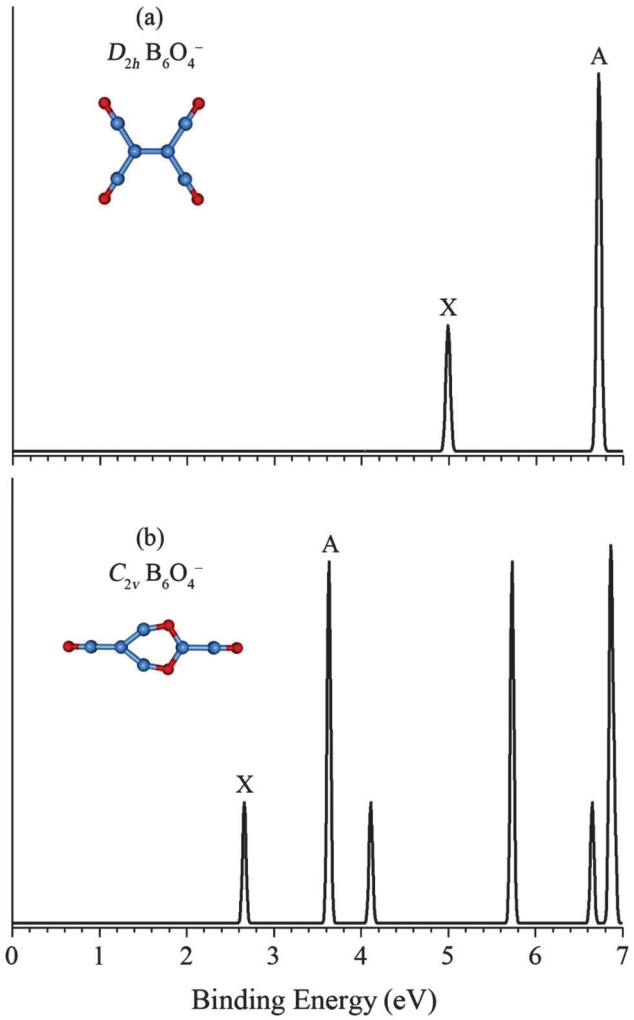

Fig. 4 Simulated photoelectron spectra of (a) the ethylene-like $B_6O_4^-$ D_{2h} (**2**, $^2B_{3u}$) cluster and (b) the benzene-like $B_6O_4^-$ C_{2v} ($^2A_1$) anion. The spectra are constructed by fitting the calculated vertical detachment energies with unit-area Gaussian functions of 0.05 eV half-width.

(Fig. S2 in the ESI†). The C_{2v} $B_6O_4^-$ ($^2A_1$) anion is experimentally not viable.

5. Conclusions

We report on theoretical prediction of a series of new boron oxide clusters: C_{2v} B_6O_4 (**1**), D_{2h} $B_6O_4^-$ (**2**), and D_{2h} $B_6O_4^{2-}$ (**3**). These perfectly planar clusters are identified as the global-minimum structures of the system *via* the coalescence kick and basin hopping global-minimum searches and electronic structure calculations at the B3LYP, CCSD, and single-point CCSD(T) levels. The B_6O_4 (**1**) cluster possesses a hexagonal B_4O_2 ring, whereas $B_6O_4^{-/2-}$ (**2** and **3**) possess ethylene-like open structures. Chemical bonding is elucidated using the canonical molecular orbital analysis, the adaptive natural density partitioning, and the nucleus independent chemical shift, which collectively show that B_6O_4 (**1**) is a new member of the inorganic benzene family, featuring a π sextet in the heterocyclic B_4O_2 ring, whereas $B_6O_4^{-/2-}$ (**2** and **3**) are boron oxide analogues of ethylene. The current results highlight the robustness of the BO group as a ligand and its isolobal analogy to H, and build intriguing connections between boron oxide clusters and hydrocarbons (C_6H_6 and C_2H_4).

Acknowledgements

This work was supported by the National Natural Science Foundation of China (21243004 and 21373130), the Shanxi International Cooperation project (2013081018), and the State Key Laboratory of Quantum Optics and Quantum Optics Devices (KF201402). H.J.Z. gratefully acknowledges the start-up fund from Shanxi University for support.

Notes and References

1 H. J. Zhai, Q. Chen, H. Bai, S. D. Li and L. S. Wang, *Acc. Chem. Res.*, 2014, **47**, 2435–2445.
2 L. Hanley and S. L. Anderson, *J. Chem. Phys.*, 1988, **89**, 2848–2860.
3 P. G. Wenthold, J. B. Kim, K. L. Jonas and W. C. Lineberger, *J. Phys. Chem. A*, 1997, **101**, 4472–4474.
4 D. Peiris, A. Lapicki, S. L. Anderson, R. Napora, D. Linder and M. Page, *J. Phys. Chem. A*, 1997, **101**, 9935–9941.
5 T. R. Burkholder and L. Andrews, *J. Chem. Phys.*, 1991, **95**, 8697–8709.
6 H. J. Zhai, L. M. Wang, S. D. Li and L. S. Wang, *J. Phys. Chem. A*, 2007, **111**, 1030–1035.
7 H. J. Zhai, S. D. Li and L. S. Wang, *J. Am. Chem. Soc.*, 2007, **129**, 9254–9255.
8 S. D. Li, H. J. Zhai and L. S. Wang, *J. Am. Chem. Soc.*, 2008, **130**, 2573–2579.
9 H. J. Zhai, J. C. Guo, S. D. Li and L. S. Wang, *ChemPhysChem*, 2011, **12**, 2549–2553.
10 Q. Chen, H. J. Zhai, S. D. Li and L. S. Wang, *J. Chem. Phys.*, 2012, **137**, 044307.
11 H. J. Zhai, Q. Chen, H. Bai, H. G. Lu, W. L. Li, S. D. Li and L. S. Wang, *J. Chem. Phys.*, 2013, **139**, 174301.
12 J. C. Guo, H. G. Lu, H. J. Zhai and S. D. Li, *J. Phys. Chem. A*, 2013, **117**, 11587–11591.
13 W. J. Tian, H. G. Xu, X. Y. Kong, Q. Chen, W. J. Zheng, H. J. Zhai and S. D. Li, *Phys. Chem. Chem. Phys.*, 2014, **16**, 5129–5136.
14 Q. Chen, H. G. Lu, H. J. Zhai and S. D. Li, *Phys. Chem. Chem. Phys.*, 2014, **16**, 7274–7279.
15 D. Y. Zubarev, A. I. Boldyrev, J. Li, H. J. Zhai and L. S. Wang, *J. Phys. Chem. A*, 2007, **111**, 1648–1658.
16 H. J. Zhai, C. Q. Miao, S. D. Li and L. S. Wang, *J. Phys. Chem. A*, 2010, **114**, 12155–12161.
17 H. Bai, H. J. Zhai, S. D. Li and L. S. Wang, *Phys. Chem. Chem. Phys.*, 2013, **15**, 9646–9653.
18 Q. Chen, H. Bai, H. J. Zhai, S. D. Li and L. S. Wang, *J. Chem. Phys.*, 2013, **139**, 044308.

19 W. Z. Yao, J. C. Guo, H. G. Lu and S. D. Li, *J. Phys. Chem. A*, 2009, **113**, 2561–2564.
20 S. D. Li, J. C. Guo and G. M. Ren, *THEOCHEM*, 2007, **821**, 153–159.
21 A. N. Alexandrova, A. I. Boldyrev, H. J. Zhai and L. S. Wang, *Coord. Chem. Rev.*, 2006, **250**, 2811–2866.
22 H. J. Zhai, L. S. Wang, A. N. Alexandrova, A. I. Boldyrev and V. G. Zakrzewski, *J. Phys. Chem. A*, 2003, **107**, 9319–9328.
23 H. J. Zhai, L. S. Wang, A. N. Alexandrova and A. I. Boldyrev, *J. Chem. Phys.*, 2002, **117**, 7917–7924.
24 A. N. Alexandrova, A. I. Boldyrev, H. J. Zhai, L. S. Wang, E. Steiner and P. W. Fowler, *J. Phys. Chem. A*, 2003, **107**, 1359–1369.
25 A. N. Alexandrova, A. I. Boldyrev, H. J. Zhai and L. S. Wang, *J. Chem. Phys.*, 2005, **122**, 054313.
26 A. N. Alexandrova, A. I. Boldyrev, H. J. Zhai and L. S. Wang, *J. Phys. Chem. A*, 2004, **108**, 3509–3517.
27 H. J. Zhai, A. N. Alexandrova, K. A. Birch, A. I. Boldyrev and L. S. Wang, *Angew. Chem., Int. Ed.*, 2003, **42**, 6004–6008.
28 A. N. Alexandrova, H. J. Zhai, L. S. Wang and A. I. Boldyrev, *Inorg. Chem.*, 2004, **43**, 3552–3554.
29 J. E. Fowler and J. M. Ugalde, *J. Phys. Chem. A*, 2000, **104**, 397–403.
30 J. Aihara, *J. Phys. Chem. A*, 2001, **105**, 5486–5489.
31 A. P. Sergeeva, D. Y. Zubarev, H. J. Zhai, A. I. Boldyrev and L. S. Wang, *J. Am. Chem. Soc.*, 2008, **130**, 7244–7246.
32 A. P. Sergeeva, B. B. Averkiev, H. J. Zhai, A. I. Boldyrev and L. S. Wang, *J. Chem. Phys.*, 2011, **134**, 224304.
33 W. Huang, A. P. Sergeeva, H. J. Zhai, B. B. Averkiev, L. S. Wang and A. I. Boldyrev, *Nat. Chem.*, 2010, **2**, 202–206.
34 B. Kiran, S. Bulusu, H. J. Zhai, S. Yoo, X. C. Zeng and L. S. Wang, *Proc. Natl. Acad. Sci. U. S. A.*, 2005, **102**, 961–964.
35 Z. A. Piazza, W. L. Li, C. Romanescu, A. P. Sergeeva, L. S. Wang and A. I. Boldyrev, *J. Chem. Phys.*, 2012, **136**, 104310.
36 A. P. Sergeeva, Z. A. Piazza, C. Romanescu, W. L. Li, A. I. Boldyrev and L. S. Wang, *J. Am. Chem. Soc.*, 2012, **134**, 18065–18073.
37 W. L. Li, Q. Chen, W. J. Tian, H. Bai, Y. F. Zhao, H. S. Hu, J. Li, H. J. Zhai, S. D. Li and L. S. Wang, *J. Am. Chem. Soc.*, 2014, **136**, 12257–12260.
38 Q. Chen, G. F. Wei, W. J. Tian, H. Bai, Z. P. Liu, H. J. Zhai and S. D. Li, *Phys. Chem. Chem. Phys.*, 2014, **16**, 18282–18287.
39 H. J. Zhai, Y. F. Zhao, W. L. Li, Q. Chen, H. Bai, H. S. Hu, Z. A. Piazza, W. J. Tian, H. G. Lu, Y. B. Wu, Y. W. Mu, G. F. Wei, Z. P. Liu, J. Li, S. D. Li and L. S. Wang, *Nat. Chem.*, 2014, **6**, 727–731.
40 Q. Chen, W. L. Li, Y. F. Zhao, S. Y. Zhang, H. S. Hu, H. Bai, H. R. Li, W. J. Tian, H. G. Lu, H. J. Zhai, S. D. Li, J. Li and L. S. Wang, *ACS Nano*, 2015, **9**, 754–760.
41 Q. Chen, S. Y. Zhang, H. Bai, W. J. Tian, T. Gao, H. R. Li, C. Q. Miao, Y. W. Mu, H. G. Lu, H. J. Zhai and S. D. Li, *Angew. Chem., Int. Ed.*, 2015, **54**, 8160–8164.
42 H. Bai, Q. Chen, H. J. Zhai and S. D. Li, *Angew. Chem., Int. Ed.*, 2015, **54**, 941–945.
43 J. I. Aihara, H. Kanno and T. Ishida, *J. Am. Chem. Soc.*, 2005, **127**, 13324–13330.
44 H. J. Zhai, B. Kiran, J. Li and L. S. Wang, *Nat. Mater.*, 2003, **2**, 827–833.
45 P. W. Fowler and E. Steiner, *J. Phys. Chem. A*, 1997, **101**, 1409–1413.
46 D. Z. Li, H. Bai, Q. Chen, H. G. Lu, H. J. Zhai and S. D. Li, *J. Chem. Phys.*, 2013, **138**, 244304.
47 G. Ferlat, T. Charpentier, A. P. Seitsonen, A. Takada, M. Lazzeri, L. Cormier, G. Calas and F. Mauri, *Phys. Rev. Lett.*, 2008, **101**, 065504.
48 J. D. Mackenzie, *J. Phys. Chem. A*, 1959, **63**, 1875–1878.
49 P. P. Bera, K. W. Sattelmeyer, M. Saunders, H. F. Schaefer and P. v. R. Schleyer, *J. Phys. Chem. A*, 2006, **110**, 4287–4290.
50 M. Saunders, *J. Comput. Chem.*, 2004, **25**, 621–626.
51 D. J. Wales and J. P. K. Doye, *J. Phys. Chem. A*, 1997, **101**, 5111–5118.
52 A. D. Becke, *J. Chem. Phys.*, 1993, **98**, 5648–5652.
53 G. E. Scuseria, C. L. Janssen and H. F. Schaefer, *J. Chem. Phys.*, 1988, **89**, 7382–7387.
54 G. E. Scuseria and H. F. Schaefer, *J. Chem. Phys.*, 1989, **90**, 3700–3703.
55 D. Y. Zubarev and A. I. Boldyrev, *Phys. Chem. Chem. Phys.*, 2008, **10**, 5207–5217.
56 P. v. R. Schleyer, C. Maerker, A. Dransfeld, H. Jiao and N. J. R. E. Hommes, *J. Am. Chem. Soc.*, 1996, **118**, 6317–6318.
57 P. V. R. Schleyer, H. Jiao, N. J. R. V. E. Hommes, V. G. Malkin and O. L. Malkina, *J. Am. Chem. Soc.*, 1997, **119**, 12669–12670.
58 M. E. Casida, C. Jamorski, K. C. Casida and D. R. Salahub, *J. Chem. Phys.*, 1998, **108**, 4439–4449.
59 M. J. Frisch, G. W. Trucks, H. B. Schlegel and G. E. Scuseria, *et al.*, GAUSSIAN 09, revision A.2, Gaussian, Inc., Wallingford, CT, 2009.
60 J. K. Olson and A. I. Boldyrev, *Chem. Phys. Lett.*, 2012, **523**, 83–86.
61 A. N. Kocharian, G. W. Fernando, K. Palandage and J. W. Davenport, *Phys. Rev. B: Condens. Matter Mater. Phys.*, 2006, **74**, 024511.
62 A. N. Kocharian, G. W. Fernando, K. Palandage and J. W. Davenport, *Phys. Rev. B: Condens. Matter Mater. Phys.*, 2008, **78**, 075431.
63 O. M. Auslaender, A. Yacoby, R. de Picciotto, K. W. Baldwin, L. N. Pfeiffer and K. W. West, *Phys. Rev. Lett.*, 2000, **84**, 1764–1767.
64 M. Sassetti and B. Kramer, *Phys. Rev. Lett.*, 1998, **80**, 1485–1488.
65 F. Lopez-Urias, E. Cruz-Silva, E. Munoz-Sandoval, M. Terrones and H. Terrones, *J. Mater. Chem.*, 2008, **18**, 1535–1541.